Femtosecond Laser Nano-Fabrication With Extended Processing Range

Zhi-Yong Hu, Yun-Lu Sun, Jian-Guan Hua, Yan-Hao Yu, Qi-Dai Chen, and Hong-Bo Sun, *Fellow, IEEE*

***Abstract*— Superior performances, such as high processing speed and resolution, make galvano-mirror-based fabricating strategy widely applied, particularly for micro/nano-scale femtosecond laser direct writing (FsLDW). However, the optically limited processing area restricts its applications. Here, we report a simple, low-cost, and universal pre-compensation method that corrected the off-axis optical aberrations to considerably expand the processing area of galvano-mirror-based nano-FsLDW with 3D nano-resolution maintained. A high-quality continuous-surface Fresnel lens was one-step fabricated with a 550-μm diameter, which surpassed the effective range (~150-μm) of the high-numerical aperture objective lens used for high resolution. It provides a significant approach for novel high-speed/efficiency micro/nano-FsLDW of diverse micro/nano-elements/systems.**

***Index Terms*— Galvano-mirror-based femtosecond laser direct writing, pre-compensation technique, processing area expansion, micro/nano-optics.**

I. Introduction

FEMTOSECOND laser direct writing (FsLDW) is an excellent 3D micro/nano fabricating technology, which has shown huge application potential in the construction of micro-optics [1], [2], micromechanics [3], microelectronics [4], [5], and microfluidics [6], [7], owing to its merits in wide material applicability, high-precision and programmable designability in 3D [1]–[11]. The FsLDW systems are mainly enabled with two scanning methods via galvanometers and/or motion stages. Besides lower cost and complexity, galvanometer-based FsLDW can be endowed with sub-nm 3D positioning accuracy, higher scanning/fabricating speed, and fast laser focus jumps (<200 μs), so the systems are widely used for the high-speed, high-efficiency machining of complex 3D structures [12], [13]. In many application cases, not only the nano-scale spatial resolution, but also a larger processing range, is highly needed [6], [7], [10]. However, due to the off-axis optical aberrations of the galvano-mirror scanning system combined with 4F imaging system and a high-NA objective lens, the processing area is optically limited. It brings challenges to realize superior processing flexibility, efficiency and quality, especially for structures with relatively large-area and nano-resolution. The field-distortion-induced errors in conventional laser galvano-mirror-based scanning systems are mainly caused by optical laser beam drift, mechanical misalignment, thermal effects, and/or installation offset [14], [15]. The hardware-based correction of one or several aspects of these systematic errors increases the cost and complexity, or even impacts other performances.

The pre-compensation modeling scheme is a facile but effective solution to the distortion of laser galvano-mirror scanning systems [14], [15]. At present, the re-calibration is mainly to correct the nonlinearity scanning distortion of the galvanometer system for 2D large-scale laser-based imaging and processing (e.g., laser marking [14], drilling [15]). Whereas, a FsLDW system usually has field distortion errors exacerbated by the off-axis optical aberrations of the 4F image system and high-NA objective lens used for tightly focusing and high resolution. The sub-micro-/nano-FsLDW also requires higher accuracy. This pre-compensation method is rarely reported in 3D micro/nano- FsLDW as far as we know. Herein, we novelly applied the pre-compensation in FsLDW structure modeling to facilely and considerably expand the processing area, and simultaneously well maintain its 3D quality and accuracy. The versatile corrections of FsLDW with different objective lenses were implemented by using similar elliptic parabola function. For 500-nm-thick 2D patterns, the effective processing range can be remarkably expanded. For 20×, 40×, 60×, and 100× objective lenses, the fabrication area was enlarged approximately by 1400%, 700%, 400%, and 100%, respectively. As a demonstration, we fabricated a continuous-surface Fresnel microlens with good 3D structural quality and optical performances. Its diameter is 550-μm, ~267% larger than the originally ~150-μm processing range of FsLDW equipped with a ~1.35-NA objective lens. In this work, the novel FsLDW with modeling compensation is proved of potential for customizing large-area 3D devices with high speed/efficiency/quality, and further facilitating its wide applications (e.g., integrated optics, microfluidics).

Manuscript received October 31, 2018; accepted November 28, 2018. Date of publication December 3, 2018; date of current version January 16, 2019. This work was supported in part by the National Key R&D Program of China under Grant 2017YFB1104600 and in part by the National Natural Science Foundation of China (NSFC) under Grant 61590930, Grant 61605055, Grant 61435005, and Grant 21473076. *(Corresponding authors: Hong-Bo Sun; Yun-Lu Sun.)*

Z.-Y. Hu, Y.-L. Sun, J.-G. Hua, Y.-H. Yu, and Q.-D. Chen are with the State Key Laboratory of Integrated Optoelectronics, College of Electronic Science and Engineering, Jilin University, Changchun 130012, China (e-mail: sunyunlu@jlu.edu.cn).

H.-B. Sun is with the State Key Laboratory of Integrated Optoelectronics, College of Electronic Science and Engineering, Jilin University, Changchun 130012, China, and also with the State Key Laboratory of Precision Measurement Technology and Instruments, Department of Precision Instrument, Tsinghua University, Beijing 100084, China (e-mail: hbsun@tsinghua.edu.cn).

Color versions of one or more of the figures in this letter are available online at http://ieeexplore.ieee.org.

Digital Object Identifier 10.1109/LPT.2018.2884568

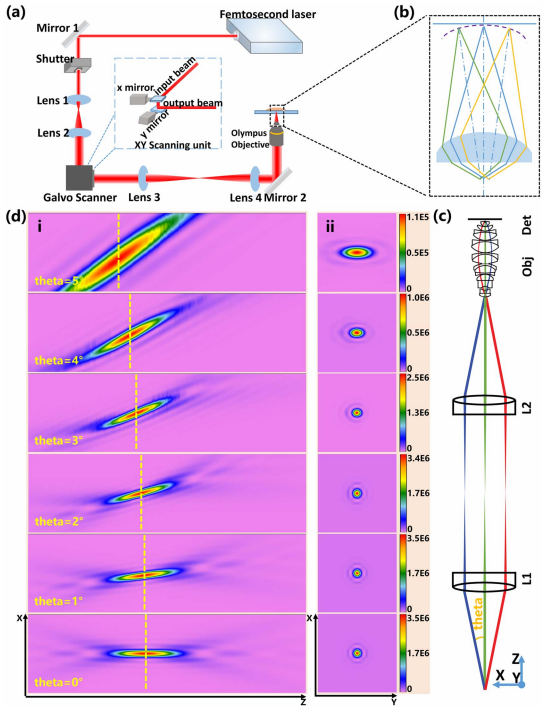

Fig. 1. (a) Femtosecond laser galvano-mirror-based 4f micro/nano processing system (Inset diagram is the schematic diagram of the scanning galvano mirror set). (b) Schematic diagram for the off-axis optical aberration of the system. (c) Schematic diagram of the simulated light path. (d) Morphologies and energy distribution of focuses at different off-axis angles. (i) is parallel and (ii) is vertical to the direction of beam propagation. Light travels along the Z axis.

II. Distortion Analysis and Modeling Pre-Compensation

Figure 1(a) shows the FsLDW micro/nano processing system (80-MHz repetition frequency, 780-nm center wavelength and 100-fs pulse width), with a schematic inset of the galvano mirror set enabling X-Y scanning of the laser beam. In the galvano-mirror-based femtosecond laser processing system, we used a 4F imaging system with a high NA objective lens instead of the traditional F-θ lens to achieve the sub-wavelength processing accuracy [16], [17]. At the entrance pupil of the objective lens, the laser beam was deflected only angularly without obvious position shift. So that the laser spot scanning was better controlled in 2D especially for relatively large-area fabrication. Combined with nano-level Z-axis sample movements via a piezo stage, 3D processing could be well implemented.

To evaluate the impact to large-area fabrication and purposely correction, the off-axis aberrations induced by the 4F system and high-NA objective lens are numerically simulated here with the light-field simulation software Virtual Lab Fusion (LightTrans, Germany) (Figure 1(c) and (d)). A simplified lens assembly of the commercial objective [18] is used for simulation, agreeing basically with the experimental results. In Figure 1(c) and (d), as the incident light angle deviated, the position of the focused spot gradually deviated from the ideal focal plane, but the spot shape remained largely unchanged at the off-axis angle within 3 degrees. The off-axis error of the entire optical system was mainly represented as image field curvature, as shown in Figure 1(b).

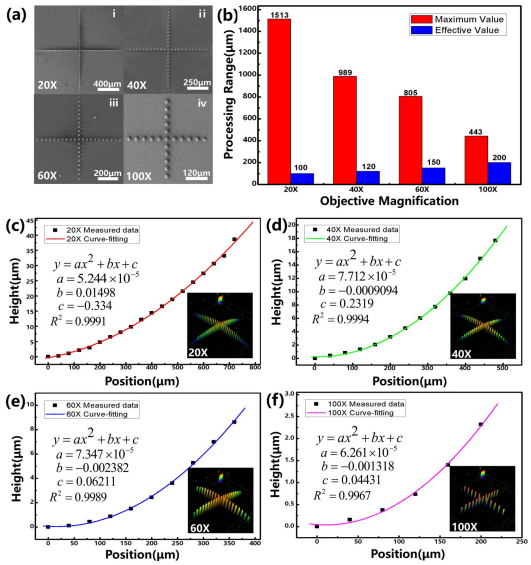

Fig. 2. (a) Scanning electron microscope (SEM) images of different cross-cylinder model structures fabricated by different objective lenses (i. 20×, ii. 40×, iii. 60×, iv. 100×). (b) Dependence of maximum and effective processing range on objective magnification. (c-f) Experimental height deviation and curve fitting dependence on the position (c. 20×, d. 40×, e. 60×, f. 100×). The insert images are the 3D morphologies of structures in (a) obtained via using laser scanning confocal microscope (LSCM).

We used the resin composed of 1wt% photoinitiator (Benzil, Aladdin) and 99wt% photoresist (NOA63, Norland Products) with a lower polymerization threshold. In Figure 2(a), the 25μm-spaced single cylinders were designed with 15-μm diameter. By fabricating these dot arrays with enough height (the heights of 20×, 40×, 60×, and 100× objectives were 45um, 25um, 20um, and 15um, respectively), we modeled the distortion function of this galvano-mirror-based FsLDW system (Figure 2(c)-(f)). The insert images in Figure 2(c)-(f) show the 3D geometry of fabricated structures via using laser scanning confocal microscope (LSCM). The distortion increased quickly along with the increase of fabrication size. For 20×, 40×, 60×, and 100× objective lenses (Olympus UPSAPO (40×, UPFLN); NA, 0.85, 1.30, 1.35, and 1.40, respectively), the maximum scanning span without considering the height error could reach approximately 1500%, 800%, 500%, and 200% of the effective fabrication range with an acceptable fabricating distortion (the height error is lower than 500 nm here), respectively (Figure 2(b)). These results show the huge potential of performance enhancement via this pre-compensation method.

The distortion of the optical field could be quantified according to the deviation between the actual height and the design value of the structure fabricated. The height deviations measured by LSCM were curve-fitted using the elliptical parabola function to obtain the pre-compensation correction curves for different objective lenses. With the coefficient of determination R^2 over 0.99, the cross-section profile of the distortion matched well with the parabolic equation (Figure 2(c)-(f)):

$$y = ax^2 + bx + c \tag{1}$$

Accordingly, the 3D fabrication could be remodeling with machining data pre-compensation, so the optically induced

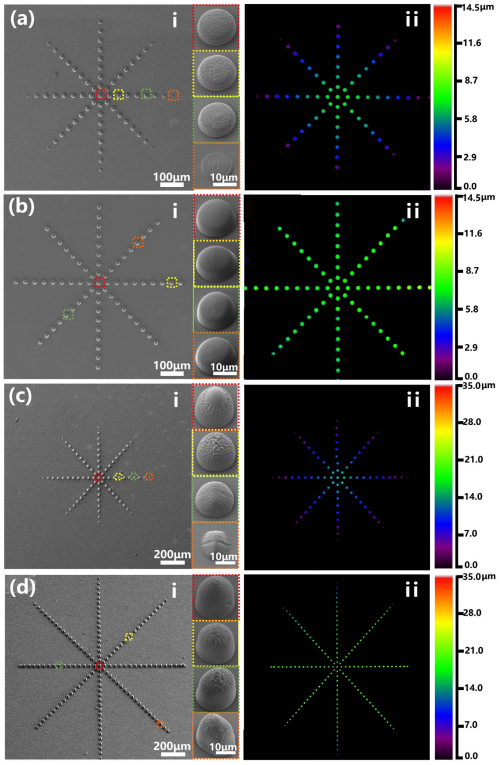

Fig. 3. Comparison of corrected and uncorrected meter-shaped cylinder array's processing results. (a) A pattern fabricated without correction by using the 60×/1.35NA objective lens. (b) The pattern in (a) fabricated with correction by using the 60×/1.35NA objective lens. (c) A pattern fabricated without correction by using the 20×/0.85NA objective lens. (d) The pattern in (c) fabricated with correction by using the 20×/0.85NA objective lens. (a)-i, (b)-i, (c)-i, (d)-i are the SEM images and (a)-ii, (b)-ii, (c)-ii, (d)-ii are the LSCM images of the structure. Enlarged-view SEM images are marked for single cylinders in different positions of the patterns.

distortion of fabrication could be corrected remarkably and facilely. The Figure 3 shows the corrected and uncorrected processing results for the 60× and 20× objective lenses. In the picture, (i) is the SEM photograph and (ii) is the LSCM image of the structure. Illustrations with different color borders are enlarged SEM pictures of single cylinder in different positions. The contrast results indicated that the processing range was limited and the structure height gradually decreases from the middle to the edge without data correction. After correction, the machining range effectively expanded and the height and morphologies of the center and the edge keep consistent. The scanning speed and single pulse energy both before and after correction were 1 mm/s and 0.35nJ. These results fully proved the effectiveness of our pre-compensation technique.

III. Fabrication Quality After Correction

The SEM image in Figure 4(a) shows lines fabricated with different scanning speeds (1.5-60 μm/s) by using the 60× lens. The minimum line width of 216 nm could be achieved, much smaller than the laser wavelength applied (780 nm). Figure 4(b) gives the relation of FsLDW resolution (i.e., line width) in the center of the fabricating view with scanning speed and pulse energy. Increasing scanning speed or decreasing single pulse energy causes smaller line width. Figure 4(c) and (d) show the fabricating resolutions under

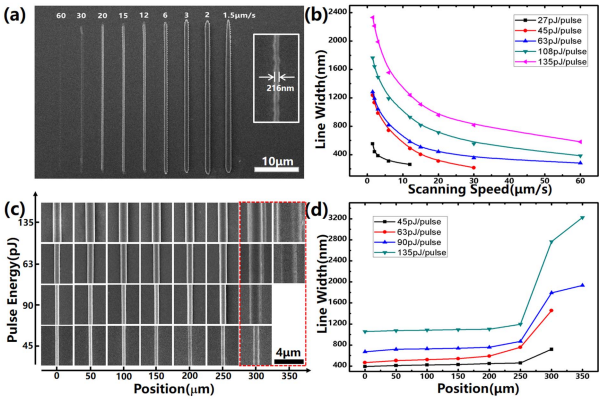

Fig. 4. Single line width at various scanning speeds, processing positions and single pulse energy conditions. (a) SEM images of the lines processed at different scanning speeds at the center of the view field. The illustration is the minimum line width of 216 nm. (b) The curve of processing line width with scanning speed under different pulse energy. (c) SEM images of the lines processed at different machining position and single pulse energy. (d) The curve of processing line width with machining position under different single pulse energy.

different single pulse energy at processing positions from the center to the edge. The processing resolution slowly increased in the range of less than 5% variation within the threshold span, beyond which it increased dramatically, which is in good agreement with the optical simulation (Figure 1(d). ii). High 3D quality and accuracy can be well maintained within this scanning span (~250μm radius for the 60× lens) with pre-compensation in FsLDW.

IV. One-Step Fabrication of Optical Elements

To prove the processing capability of the rectified processing system, we designed and fabricated a large-size continuous-surface Fresnel lens. The Fresnel lens configuration was obtained by quantizing the phase of a spherical lens. It had the advantages like relatively small size and weight, and easy integration [19], [20]. The relationship between the optical path difference and the phase difference was:

$$\Delta\varphi = \Delta n \mathrm{h} \cdot \frac{2\pi}{\lambda} \tag{2}$$

The refractive index n of the polymer material was 1.56 and the designed device had a test wavelength of 633 nm. Taking into account the processing morphology of the device, we let $\Delta\varphi$ equals to 6π for quantification, so the height of the sawtooth could be obtained as 3.39μm. According to the high-precision processing range threshold obtained in the previous experiments, we designed the device with a diameter of 550μm. Considering the aesthetics and rationalization of the device, the spherical lens was quantified into 18 layers of sawtooth. According to the thin lens equation:

$$f = f' = \frac{1}{(n_L - 1)(\frac{1}{r_1} - \frac{1}{r_2})} \tag{3}$$

The focal length of the spherical lens was calculated to be 1161μm. The experimental result (~1150μm) was approximately consistent with the theoretical design.

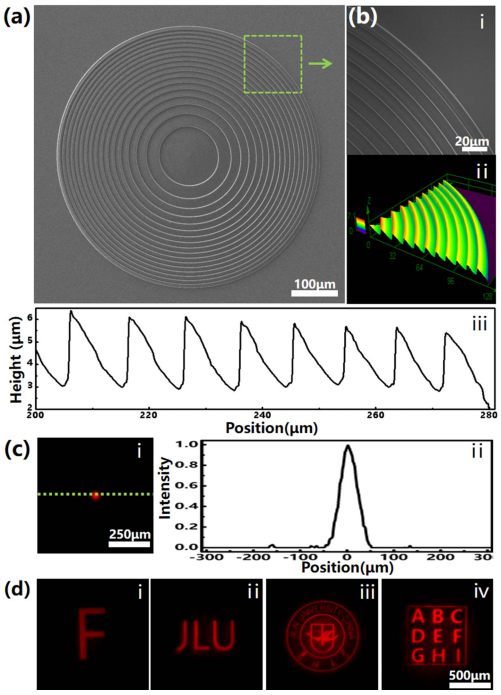

Fig. 5. Fabrication of large-size continuous surface Fresnel Lens. (a) The SEM image of the continuous surface Fresnel Lens. (b) Local magnification of selected area in (a). (i) is the SEM photograph, (ii) is the 3D LSCM image and (iii) is the height contour extraction of the structure. (c) Focus test. (i) is the focused spot shape and (ii) is light intensity spatial distribution curve at green dotted line. (d) Different pattern optical imaging test.

Figure 5(a) shows the SEM image of the as-fabricated continuous surface Fresnel lens. High 3D structural and morphological qualities were proved as shown in Figure 5(b). The continuous surface had an as-designed cross-section profile. With a 550-μm diameter (about 4 times of original fabrication span before correction), this lens was of as-designed constant height and 3D configuration from the center to the edge. For the optical properties of the Fresnel lens, Figure 5(c) shows the spot size and spatial distribution of the light intensity at the focal spot. Figure 5(d) shows its superior focusing and imaging. The purposely field curvature correction improves the FsLDW fabrication of large-scale micro/nano-devices.

V. Conclusion

In summary, we used a simple and universal method to correct the error of the 4f galvano-mirror-based scanning FsLDW system by the pre-compensation method, and realized the high-speed and high-precision one-step processing of micro/nano-optics with relatively large size. On the premise of guaranteeing the processing accuracy especially in the edge area, a continuous-surface Fresnel lens was well customized for demonstration by using a high-NA objective lens. It had a 550-μm diameter ~267% larger than the effective fabricating range of the FsLDW before correction, and superior 3D structural quality and optical performances. Our work provided a facile and versatile method for micro/nano-FsLDW improved with high speed, efficiency and quality (also applicable for other direct-writing techniques), facilitating the construction of diverse micro/nano-scale elements and systems for wider applications (e.g., lab on a chip, integrated optics and/or photonics).

References

[1] G. Li, K. A. Winick, A. A. Said, M. Dugan, and P. Bado, "Waveguide electro-optic modulator in fused silica fabricated by femtosecond laser direct writing and thermal poling," *Opt. Lett.*, vol. 31, no. 6, pp. 739–741, Mar. 2006.

[2] S. Fischbach *et al.*, "Single quantum dot with microlens and 3D-printed micro-objective as integrated bright single-photon source," *ACS. Photon.*, vol. 4, no. 6, pp. 1327–1332, May 2017.

[3] M. Malinauskas *et al.*, "3D microporous scaffolds manufactured via combination of fused filament fabrication and direct laser writing ablation," *Micromachines*, vol. 5, no. 4, pp. 839–858, Sep. 2014.

[4] X. Zang *et al.*, "Laser-induced molybdenum carbide–graphene composites for 3D foldable paper electronics," *Adv. Mater.*, vol. 30, no. 26, p. 1800062, Feb. 2018.

[5] A. Wang *et al.*, "Mask-free patterning of high-conductivity metal nanowires in open air by spatially modulated femtosecond laser pulses," *Adv. Mater.*, vol. 27, no. 40, pp. 6238–6243, Sep. 2015.

[6] Y. Ju *et al.*, "Direct fabrication of a microfluidic chip for electrophoresis analysis by water-assisted femtosecond laser writing in porous glass," *Chin. Opt. Lett.*, vol. 11, no. 7, p. 072201, Jul. 2013.

[7] K. Sugioka, Y. Cheng, and K. Midorikawa, "Three-dimensional micromachining of glass using femtosecond laser for lab-on-a-chip device manufacture," *Appl. Phys. A*, vol. 81, no. 1, pp. 1–10, Apr. 2005.

[8] W. Wang *et al.*, "Direct laser writing of superhydrophobic PDMS elastomers for controllable manipulation via marangoni effect," *Adv. Funct. Mater.*, vol. 27, no. 44, p. 1702946, Jul. 2017.

[9] G. Fang, H. Cao, L. Cao, and X. Duan, "Femtosecond laser direct writing of 3D silica-like microstructure from hybrid epoxy cyclohexyl POSS," *Adv. Mater. Technol.*, vol. 3, no. 3, p. 1700271, Mar. 2018.

[10] L. Wang *et al.*, "Plasmonic nano-printing: Large-area nanoscale energy deposition for efficient surface texturing," *Light, Sci. Appl.*, vol. 6, no. 12, pp. e17112, Dec. 2017.

[11] M. Malinauskas *et al.*, "Ultrafast laser processing of materials: from science to industry," *Light, Sci. Appl.*, vol. 5, no. 8, p. e16133, Aug. 2016.

[12] H. Wang *et al.*, "Femtosecond laser direct writing of ion exchangeable multifunctional microstructures," *Opt. Lett.*, vol. 43, no. 5, pp. 1139–1142, Feb. 2018.

[13] Z. Cai *et al.*, "Continuous cubic phase microplates for generating high-quality airy beams with strong deflection," *Opt. Lett.*, vol. 42, no. 13, pp. 2483–2486, Jun. 2017.

[14] J. Xie, S. Huang, Z. Duan, Y. Shi, and S. Wen, "Correction of the image distortion for laser galvanometric scanning system," *Opt. Laser Technol.*, vol. 37, no. 4, pp. 305–311, Apr. 2005.

[15] M.-F. Chen and Y.-P. Chen, "Compensating technique of field-distorting error for the CO_2 laser galvanometric scanning drilling machines," *Int. J. Mach. Tool Manuf.*, vol. 47, nos. 7–8, pp. 1114–1124, Oct. 2007.

[16] W. Han, W. Cheng, and Q. Zhan, "Design and alignment strategies of $4f$ systems used in the vectorial optical field generator," *Appl. Opt.*, vol. 54, no. 9, pp. 2275–2278, Mar. 2015.

[17] J. W. Pyhtila and A. Wax, "Improved interferometric detection of scattered light with a $4f$ imaging system," *Appl. Opt.*, vol. 44, no. 10, pp. 1785–1791, Apr. 2005.

[18] T. Suzuki, "Immersion microscope objective," U.S. Patent 5 517 360 A, May 14, 1996.

[19] Y. Li *et al.*, "High efficiency multilevel phase-type Fresnel zone plates produced by two-photon polymerization of SU-8," *J. Opt.*, vol. 12, no. 3, p. 035203, Jan. 2010.

[20] P. Srisungsitthisunti, O. K. Ersoy, and X. Xu, "Volume Fresnel zone plates fabricated by femtosecond laser direct writing," *Appl. Phys. Lett.*, vol. 90, no. 1, p. 011104, Jan. 2007.